

Ray-traced tropospheric slant delays in VLBI analysis



Vahab Nafisi, Matthias Madzak, Johannes Böhm, Harald Schuh and Alireza A. Ardalan

Abstract

Modeling troposphere delays is a major source of error in the analysis of observations from space geodetic techniques, such as Very Long Baseline Interferometry (VLBI). Numerical weather models (NWM) have been continuously improving with regard to spatial and temporal resolution as well as advances in data assimilation and thus provide valuable datasets for atmospheric research. The improved accuracy of NWMs have made ray-tracing a suitable technique to estimate the slant total delays for the observations in the neutral atmosphere, i.e. mainly in the troposphere. We have developed a direct ray-tracing method for estimating those slant delays for radio signals using data of the European Centre for Medium-range Weather Forecasts (ECMWF) which is based on the solution of the Eikonal equation. We show results for a two-week campaign of continuous VLBI sessions in 2008 (CONT08), where we applied ray-traced delays to the observed delays and analyzed the repeatability of baseline lengths in comparison to a standard approach with zenith delays and mapping functions. We find that on average, baseline length repeatabilities are similar if residual zenith delays and gradients are estimated. On the other hand, as expected, ray-traced delays perform better if residual zenith delays and gradients are not solved for in VLBI analysis.

Keywords: Ray-tracing, CONT08, Tropospheric delay, Refractivity

Kurzfassung

Die Modellierung der troposphärischen Laufzeitverzögerung ist eine der Hauptfehlerquellen für die Auswertung von Beobachtungen geodätischer Weltraumverfahren wie der Very Long Baseline Interferometry (VLBI). Numerische Wettermodelle wurden in den vergangenen Jahren hinsichtlich ihrer räumlichen und zeitlichen Auflösung sowie bezüglich ihrer Genauigkeit verbessert, und dadurch eignen sie sich sehr gut für die Atmosphärenforschung. Zum Beispiel können numerische Wettermodelle dafür verwendet werden, Strahlverfolgung (Ray-tracing) zu rechnen, um die troposphärische Laufzeitverzögerung zu bestimmen. Wir haben einen Algorithmus für direktes Ray-tracing entwickelt, um diese Laufzeitverzögerungen von Signalen im Radiowellenbereich mit Hilfe von Wetterdaten des European Centre for Medium-Range Weather Forecasts (ECMWF) zu berechnen, wobei der Ray-tracing Algorithmus auf einer Lösung der Eikonal-Gleichung basiert. Gezeigt werden Ergebnisse in Form von Wiederholbarkeiten der Basislinienlängen einer zweiwöchigen kontinuierlichen VLBI-Beobachtungskampagne im Jahr 2008 (CONT08). Die erhaltenen Basislinienlängen, abgeleitet mit Verwendung der Laufzeitverzögerungen aus Ray-tracing, werden mit jenen verglichen, die Laufzeitverzögerungen eines Standardansatzes verwenden. Der Standardansatz beschreibt die Modellierung der schrägen Laufzeitverzögerung als Produkt einer Zenitlaufzeitverzögerung und einer Projektionsfunktion. Die erhaltenen Wiederholbarkeiten zeigen ähnliche Werte für die beiden Modellierungsmöglichkeiten, wenn Zenitlaufzeitverzögerungen und Gradienten in der Auswertung mitgeschätzt werden. Allerdings werden bessere Ergebnisse mit Ray-tracing erzielt, wenn diese beiden Größen in der Ausgleichung nicht geschätzt werden.

Schlüsselwörter: Strahlverfolgung, CONT08, Troposphärische Laufzeitverzögerung, Refraktivität

1. Introduction

The troposphere is a composition of dry gases and water vapor, which imposes a time delay of propagating electromagnetic waves. Furthermore, an inhomogeneous medium causes an electromagnetic (EM) wave to propagate along a curved path, which is called the bending effect. Because of these two effects on space geodetic observations, the observed distances will be longer than the straight line distances between the receiver and transmitter in vacuum. In this

paper, the combination of both effects will be called the total delay.

Tropospheric delay modeling has always been an important issue in space geodetic data analysis. As described by the IERS Conventions 2010 (Petit and Luzum, 2010 [1]) a priori hydrostatic zenith delays are usually determined from the surface pressure as suggested by Saastamoinen (1972 [2]), which are then mapped down to the elevation of the observation with the hydrostatic mapping function (Davis et. al., 1985 [6]),

while wet zenith delay parameters are estimated with the wet mapping function as partial derivative. Tropospheric gradient effects are estimated to account for the azimuthal asymmetry of the delays (Chen and Herring, 1997 [3]). Modern mapping functions such as the Vienna Mapping Functions 1 (VMF1; Böhm et al., 2006a [4]) and the Global Mapping Functions (GMF, Böhm et al., 2006b [5]) are based on numerical weather models (NWMs). In particular with the VMF1, the variability of the coefficients with respect to location of the site and time of observation is accounted by 6-hourly meteorological data sets provided by the European Centre for Medium-range Weather Forecasts (ECMWF).

NWMs have been continuously improving with regard to their spatial and temporal resolution as well as with regard to advances in data assimilation. This enhanced accuracy of NWMs has made ray-tracing a promising technique to determine the total delay.

This paper discusses the application of the ray-tracing method for calculating total tropospheric delays in VLBI analysis. In Section 2 we introduce the refractivity of moist air. In Section 3 the ray-tracing method will be discussed, which is developed for total delay computations in two dimensions. In Section 4 we show some results about applying ray-traced delays in CONT08 VLBI analysis. Outlook and concluding remarks from this research are summarized in Section 5.

2. Refractive index of moist air

For a medium, the refractive index n is defined as the ratio of the velocity of an electromagnetic wave in vacuum to the speed of propagation in this medium as stated in Equation (1)

$$n = \frac{c}{v}, \quad (1)$$

where c and v are phase velocities in vacuum and in the medium, respectively. The refractive index of a signal in moist air is slightly different from unity, and $(n-1)$ is small. Therefore, it is more convenient to introduce and use another parameter named refractivity N with $N = (n-1) \times 10^6$. The refractivity N of moist air is expressed as (Davis, 1986 [7])

$$N = k_1 \frac{p}{T} + \left(k_2' \frac{e}{T} + k_3' \frac{e}{T^2} \right) Z_v^{-1} = N_h + N_{nh}, \quad (2)$$

where k_2' is

$$k_2' = k_2 - k_1 \frac{R_d}{R_v} \quad (3)$$

and Z_v is the water vapor compressibility factor, which in normal conditions is close to one (Kleijer, 2004 [11]).

The parameters p , T , and e are total pressure, temperature, and water vapor pressure, respectively. Additionally, we need the gas constants for dry air (R_d) and water vapor (R_v). The parameters k_1 , k_2 and k_3 are refractivity coefficients; for these investigations we have used the 'best average' coefficients suggested by Rieger (2002 [8]), which are $k_1 = 77.6890 \times 10^{-2} \text{K/hPa}$, $k_2 = 71.2952 \times 10^{-2} \text{K/hPa}$, and $k_3 = 375.463 \times 10^3 \text{K}^2/\text{Pa}$.

3. Total tropospheric delay

The total delay can be defined as the difference between the propagation time of a specific wave in a real medium (in our case the troposphere), and in vacuum. In ideal conditions, which means without any dispersion, the path of the ray between the receiver and the source of the wave (a quasar in VLBI) will be a straight line.

$$S = \int_V ds. \quad (4)$$

On the other hand, due to variations in the tropospheric refractive index, the real path of the ray is defined as

$$L = \int_T n(r, \theta, \lambda, t) ds, \quad (5)$$

where r is the radial distance, θ is the co-latitude, and λ is the longitude ($0 \leq \theta \leq \pi$, $0 \leq \lambda \leq 2\pi$). $n(r, \theta, \lambda, t)$ describes the dependency of refractivity on the position of the site and also on the time of observation. Using Equations (4) and (5) and considering refractivity instead of index of refractivity, the total tropospheric delay reads as

$$\Delta\tau = 10^{-6} \int_T N(r, \theta, \lambda, t) ds + \left(\int ds - S \right). \quad (6)$$

The first term of Equation (6) represents the signal delay along the path, which causes the excess of the path. The second term denotes the so-called geometric delay. The first term inside the bracket is along the curved path T . Note that the bending effect is not synonymous with the geometric delay, since the along-path delay is evaluated along the bent ray path. Inserting Equation (2) into Equation (6), we have

$$\Delta\tau = 10^{-6} \int_T N_h(r, \theta, \lambda, t) ds + \quad (7)$$

$$+ 10^{-6} \int_T N_{nh}(r, \theta, \lambda, t) ds + \left(\int_T ds - S \right) \text{ or} \quad (8)$$

$$\Delta\tau = \Delta\tau_h + \Delta\tau_{nh} + \Delta\tau_b.$$

Equation (8) shows the different components of the signal delay due to tropospheric propagation effects, i.e. the hydrostatic ($\Delta\tau_h$) and non-hydrostatic ($\Delta\tau_{nh}$) parts as well as the bending effect $\Delta\tau_b$, which depends on total refractivity. The propagation path is also determined by the total refractivity. The total tropospheric delay can be determined by direct ray-tracing using the well known Eikonal equation, which can be expressed as (Wheelon 2001 [9])

$$|\nabla L_i|^2 = n(r, \theta, \lambda, t)^2. \quad (9)$$

In this equation ∇L_i shows the components of the ray directions and L is the optical path length. Equation (9) is a partial differential equation of the first order for $n(r, \theta, \lambda, t)$ and it can be expressed in many alternative forms. In the 3D case there are seven partial derivative equations, and six of them must be solved simultaneously and the seventh equation is Equation (5) (Cerveny, 2005 [10]). Tropospheric ray-tracing mainly deals with the determination of total delays along the ray path and thus one parameter of interest is the arc-length along the ray. The final output of this equations system will be the position of any point along the trajectory of the ray. In addition we must mention that our method is developed in orthogonal spherical coordinates, which is more suitable and meaningful for our purpose, but ray-tracing systems can be expressed and solved in any curvilinear coordinate system, including non-orthogonal systems.

Equation (9) can be easily reduced to 2D ray-tracing by neglecting out of plane components of the ray path. In this case, we assume that the ray will stay in a plane of constant azimuth.

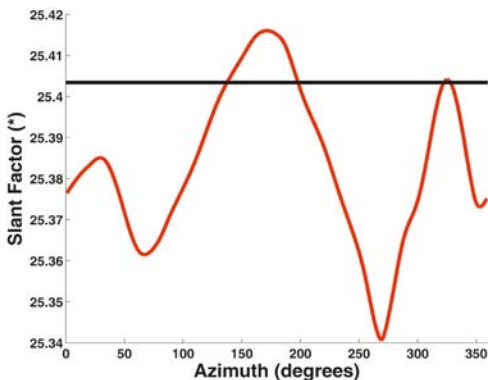


Fig. 1: Slant factors for 5 degrees elevation using the ray-tracing package (red) and VMF1 (black) for the station Tsukuba, on 18 August 2008. (*) Ray-traced slant factors are multiplied by the nominal value 2.5 m.

For our ray-tracing system we use pressure level data from the European Centre for Medium-range Weather Forecasts (ECMWF). The resolution of the dataset is 0.5 degrees and 25 pressure levels have been interpolated and extrapolated to provide reasonable incremental step sizes for solving the Eikonal Equation (9) as well as the numerical integration in Equation (7). Coordinates of the site, time of the observation and outgoing elevation angle and azimuth of the ray are other important inputs to a typical ray-tracing software. Outputs of this method are the total delays of the observations, which are used as an input to the VLBI software. Figure 1 shows the slant factors (slant total delays divided by zenith total delays) from ray-tracing as well as for VMF1.

4. Data analysis using CONT08 observations

The ray-traced tropospheric delays are included in the analysis of VLBI observations of CONT08, a two-week VLBI campaign in August 2008. For this purpose the Vienna VLBI Software (VieVS) has been adopted to read external files with the ray-traced delays. The criterion for the validity of this approach is the baseline length repeatability, i.e., the standard deviation of baseline lengths in the case of CONT08. The results are compared to those of a standard approach where a priori total delays are set up as the sum of hydrostatic and wet slant delays, each of them being the product of the zenith delay derived from data of the ECMWF and the respective VMF1 (Böhm et al., 2006a [4]). Thus in both cases, ray-tracing and ECMWF/VMF1, the a priori delays include the wet part, and if residual zenith delays are estimated the wet VMF1 is used as partial derivative with ECMWF/VMF1 and the wet Global Mapping Function (GMF, Boehm et al., 2006b [5]) with ray-tracing. We have considered three cases:

4.1 Estimating zenith delays and gradients

Figure 2 shows the baseline length repeatabilities for all baselines of the CONT08 experiment using the two models. Gradients are estimated in the analysis as well as wet zenith delays

For 31 of all 55 baselines the repeatability is better if using ECMWF/VMF1. The maximum degradation using ray-traced delays instead of ECMWF/VMF1 is 2.4 mm whereas the mean degradation is $0.6 \text{ mm} \pm 0.6 \text{ mm}$. On the other hand the remaining 24 baselines show a smaller (better) repeatability using ray-traced delays: the maximum improvement is 2.2 mm with an average of $0.5 \text{ mm} \pm 0.6 \text{ mm}$. Station TIGO is part

of the two baselines showing the maximum improvement and the maximum degradation. This cannot be explained and further investigations must be done. However, the smaller number of observations at TIGO can be a contributing reason.

4.2 Estimating zenith delays, not estimating gradients

Another analysis was carried out without estimating gradients. Since ray-tracing solves the Eikonal equation, atmospheric asymmetry is already taken into account in this method. On the other hand the model ECMWF/VMF1 calculates the total delay as a product of zenith delays and mapping functions and therefore does not consider the azimuthal asymmetry of the atmosphere. Repeatabilities are shown in Figure 3.

Baselines shorter than about 6000 km show clearly better results using ray-tracing instead of ECMWF/VMF1. In total, 36 of 55 baselines show smaller repeatabilities using ray-traced delays compared to delays from the second model. The benefit becomes smaller for longer baselines and, for most baselines longer than about 9000 km, ECMWF/VMF1 models the tropospheric path delay more accurately than ray-tracing. The differences of repeatabilities of the two models increase without estimating gradients.

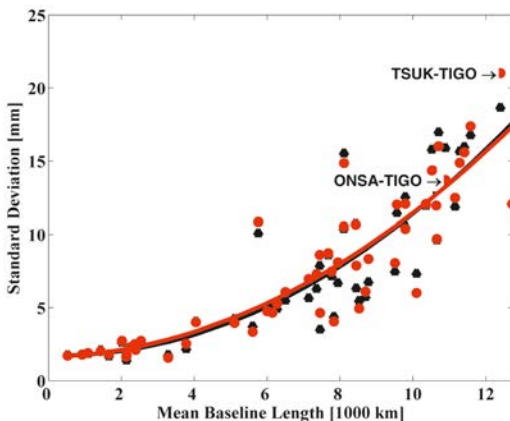


Fig. 2: Baseline length repeatabilities for CONT08 using ray-traced delays (black plus signs) and delays from the ECMWF/VMF1 (red triangles) versus baseline lengths. The solid lines show least squares polynomial curves of second order for both models for better comparability. Residual zenith delays and gradients are estimated. Two baselines showing the maximum degradation (Tsukuba-TIGO) and the maximum improvement (Onsala-TIGO), respectively, if ray-traced delays were used, are marked separately (arrows).

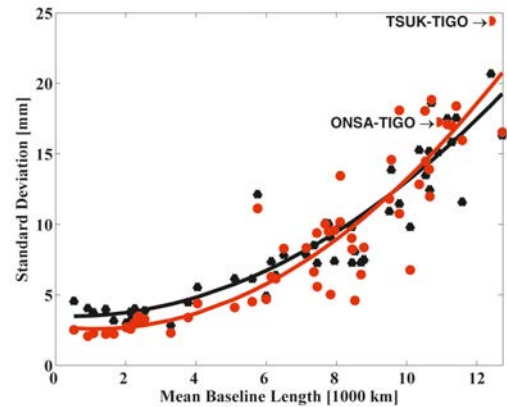


Fig. 3: Baseline length repeatabilities for CONT08 using ray-traced delays (black plus signs) and delays from ECMWF/VMF1 (red triangles) versus baseline lengths. Residual zenith delays were estimated, but no gradients. The solid lines show least squares polynomial curves of second order for both models.

4.3 Neither estimating zenith delays, nor estimating gradients

Wet zenith delays are usually estimated in the analysis as mentioned before. As both models already contain the wet part in their total delay, the additional estimation of a residual zenith delay might be unnecessary. However, in a third run baseline length repeatabilities are obtained without estimating gradients and without estimating residual zenith delays (Figure 4).

Repeatabilities increase significantly for both models compared to the results displayed in

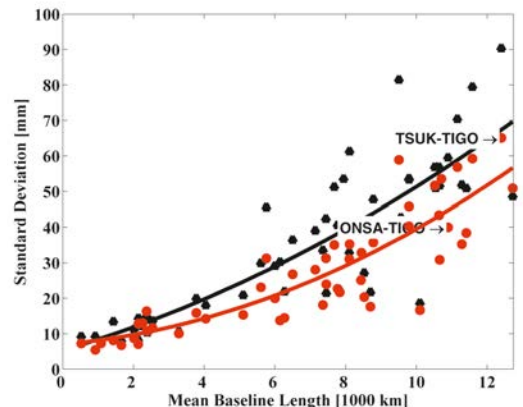


Fig. 4: Baseline length repeatabilities for CONT08 using ray-traced delays (black plus signs) and delays from ECMWF/VMF1 (red triangles). No gradients and no wet zenith delays were estimated in the analysis. The solid lines show least squares polynomial curves of second order for both models.

Figure 3. This shows clearly that residual zenith delays should be estimated also when using ray-traced delays. With ray-traced delays results are better compared to ECMWF/VMF1: 50 of 55 baselines (91%) show smaller standard deviations with ray-tracing. The mean improvement using ray-traced delays instead of ECMWF/VMF1 is 9.5 mm.

5. Concluding remarks

Ray-traced delays, obtained from the equation system shown in Section 3, were used to correct VLBI observations for the influence of the troposphere. Their quality was assessed by comparing baseline length repeatabilities for CONT08 to those derived from a standard approach with elevation-dependent mapping functions. The conclusions are: (1) On average, ray-traced delays yield an accuracy similar to the standard approach. However, taking a closer look, at some stations ray-traced delays provide better tropospheric corrections, whereas at other stations the corrections are worse compared to standard elevation-dependent models. To find the reason, more investigations need to be carried out. (2) In both cases the additional estimation of gradients and residual zenith delays is considered necessary since it improves the results.

Acknowledgments

We like to thank the International VLBI Service for Geodesy and Astrometry (IVS) (Schlüter and Behrend 2007 [12]) for coordinating the CONT08 campaign.

J. Böhm thanks the Zentralanstalt für Meteorologie und Geodynamik (ZAMG) for granting access to data of the ECMWF.

V. Nafisi thanks the Austrian Science Fund (FWF) for supporting this research under project P20902-N10 (GGOS Atmosphere). V. Nafisi would also like to acknowledge the Iran Ministry of Science, Research and Technology (MSRT) and the University of Isfahan for funding part of his research at Vienna University of Technology.

References

- [1] Petit, G. and B. Luzum, (Eds.) (2010). *IERS Conventions (2010)*. Frankfurt am Main: Verlag des Bundesamts für Kartographie und Geodäsie, Frankfurt, ISBN 1019-4568, IERS Technical Note 36, pp. 179.
- [2] Saastamoinen, J. (1972). *Atmospheric correction for the troposphere and stratosphere in radio ranging of satellites*. In *The Use of Artificial Satellites for Geodesy*, eds. S. W. Henriksen, A. Mancini, and B. H. Chovitz, Vol. 15 of *Geophysical Monograph Series*, American Geophysical Union, Washington, D.C., ISBN 0-87590-015-1, 247–251.
- [3] Chen, G. and T.A. Herring (1997), *Effects of atmospheric azimuthal asymmetry on the analysis of space geodetic data*. *J. Geophys. Res.*, 102(B9), 20489–20502.
- [4] Böhm, J., B. Werl, and H. Schuh (2006a), *Tropospheric mapping function for GPS and very long baseline interferometry from European Center for Medium-range Weather Forecasts operational analysis data*. *J. Geophys. Res.*, 111, B02406, doi:10.1029/2005JB003629.
- [5] Böhm, J., A. Niell, P. Tregoning, and H. Schuh (2006b), *The Global Mapping Function (GMF): A new empirical mapping function based on data from numerical weather model data*. *Geophys. Res. Lett.*, 33, L07304, doi:10.1029/2005GL025546.
- [6] Davis, J.L., T. A. Herring, I. I. Shapiro, A. E. E. Rogers, and G. Elgered (1985), *Geodesy by radio interferometry: Effects of atmospheric modeling errors on estimates of baseline length*, *Radio Science*, Vol. 20, No. 6, pp. 1593–1607.
- [7] Davis, J.L. (1986), *Atmospheric propagation effects on radio interferometry*. Ph. D. thesis, Harvard College Observatory, Massachusetts Institute of Technology, USA. <http://hdl.handle.net/1721.1/27953>
- [8] Rüeeger, J.M. (2002). *Refractive index formulae for radio waves*. FIG XXII International Congress, International Federation of Surveyors (FIG), Washington, D.C., http://www.fig.net/pub/fig_2002/Js28/JS28_rueger.pdf.
- [9] Wheelon, A.D. (2001), *Electromagnetic scintillation : Geometrical optics*. Cambridge University Press, pp 455.
- [10] Cerveny V. (2005), *Seismic ray theory*, Cambridge University Press, New York, pp 713.
- [11] Kleijer F., (2004), *Tropospheric Modeling and Filtering for Precise GPS Leveling*, PhD Thesis, TU Delft, pp. 262. http://enterprise.lr.tudelft.nl/publications/files/ae_kleijer_20040413.pdf
- [12] Schlüter W, Behrend D (2007) *The International VLBI Service for Geodesy and Astrometry (IVS): current capabilities and future prospects*. *J Geodesy*, 81(6–8): 379–387. doi:10.1007/s00190-006-0131-z.

Contacts

Vahab Nafisi, Institute of Geodesy and Geophysics, Vienna University of Technology, Austria; Department of Surveying and Geomatics Engineering, College of Engineering, University of Tehran, Iran; Department of Surveying Engineering, Faculty of Engineering, The University of Isfahan, Iran.

E-mail: vahab.nafisi@tuwien.ac.at, nafisi@eng.ui.ac.ir

Matthias Madzak, Institute of Geodesy and Geophysics, Vienna University of Technology, Austria.

E-mail: matthias.madzak@tuwien.ac.at

Johannes Böhm, Institute of Geodesy and Geophysics, Vienna University of Technology, Austria.

E-mail: johannes.boehm@tuwien.ac.at

Harald Schuh, Institute of Geodesy and Geophysics, Vienna University of Technology, Austria.

E-mail: harald.schuh@tuwien.ac.at

Alireza A. Ardalan, Department of Surveying and Geomatics Engineering, College of Engineering, University of Tehran, Iran.

E-mail: ardalan@ut.ac.ir